

# Influence of Hydrogen on the Structure of Cerium Films Obtained by Magnetron Sputter Deposition on Semiconductor Wafers

V. N. Verbetskii<sup>a, \*</sup>, S. V. Mitrokhin<sup>a</sup>, G. A. Badun<sup>a</sup>, S. A. Evlashin<sup>b</sup>, A. A. Tepanov<sup>a</sup>, and V. A. Bunyaev<sup>a</sup>

<sup>a</sup>Moscow State University, Moscow, 119991 Russia

<sup>b</sup>Skolkovo Institute of Science and Technology, Skoltech Center for Design, Manufacturing and Materials, Moscow 121205 Russia

\*e-mail: verbetsky@hydride.chem.msu.ru

Received September 16, 2019; revised September 30, 2019; accepted October 22, 2019

**Abstract**—The influence of hydrogen on the structure of thin cerium films formed by the method of magnetron sputter deposition was investigated in this work. Hydrogen-charging of the films was carried out by the method of Langmuir hydrogen dissociation on a tungsten substrate. The cerium hydride films were coated with a protective layer of nickel or chromium. It is demonstrated in this work that the used method of hydrogen charging can be used for introduction of hydrogen also into other hydride-forming metals and alloys.

**Keywords:** magnetron sputter deposition, rare earth metals, thin films, cerium hydride

**DOI:** 10.1134/S2075113320040425

## INTRODUCTION

Thin films based on metal hydrides and intermetallic compounds draw the particular attention of researchers owing to the possibility of their application in several branches of engineering as hydrogen sensing materials [1], electrochemical cells [2], and hydrogen storage [3]. One of the most widely used methods of formation of metal films is the magnetron sputter deposition on a substrate (physical vapor deposition). The vapor-phase hydrogen-charging or electrochemical method was earlier used to form the hydride phases based on such films. In this work, the Langmuir dissociation of hydrogen into atoms on tungsten wire was applied to form the cerium hydride films deposited on silicon wafers and coated with a protective layer of nickel or chromium. Currently, such method of obtaining of the monatomic tritium is used for introduction of the radioactive label into carbon nanomaterials and organic compounds [4–6].

### *Reagents and Materials*

Cerium (99.99%) was used in the experiments on the deposition. The metal was deposited on cleaned and degreased silicon wafers  $0.6 \times 0.6 \text{ cm}^2$  in size.

## EXPERIMENTAL

### *Magnetron Sputter Deposition*

The engineered magnetron sputtering system with two magnetrons was used for cerium deposition [7].

The sputtering was carried out from the cerium target. First, the system was exhausted to the pressure of  $10^{-5}$  Torr, and then it was filled with the working gas (99.9998% purity Ar). The working pressure was  $5 \times 10^{-2}$  Torr. Sputtering of the target was carried out at constant current. The power of energy per unit area of the surface of target, was  $1.6 \text{ W/cm}^2$  during the sputtering, which corresponded to the sputtering rate of  $0.75 \text{ nm/s}$ . Films  $300 \text{ nm}$  thick were deposited. In order to prevent oxidation of the material, the investigated film was covered with a chromium layer  $70 \text{ nm}$  thick or a nickel layer  $20 \text{ nm}$  thick.

### *Hydrogen-Charging Technique*

The samples of silicon wafers with the deposited cerium layer with the chromium or nickel coating were treated with hydrogen atoms obtained at dissociation on the tungsten wire. For that to happen, the samples were placed in a special cylindrical reservoir along the axis of which the tungsten wire was placed. The sputtering system was exhausted to the residual pressure of  $10^{-5}$  Torr and then filled with hydrogen to  $0.01$ – $0.05$  Torr, and the reaction was activated by heating the tungsten wire to  $2000 \text{ K}$  by electric current pulses for  $20 \text{ s}$  each. Periodically, the residual gas was removed and new portion of hydrogen was admitted. The total time of treatment of the samples with atomic hydrogen was  $9 \text{ min}$ . Variation of the pressure in the system was determined by a thermocouple vacuum gauge.

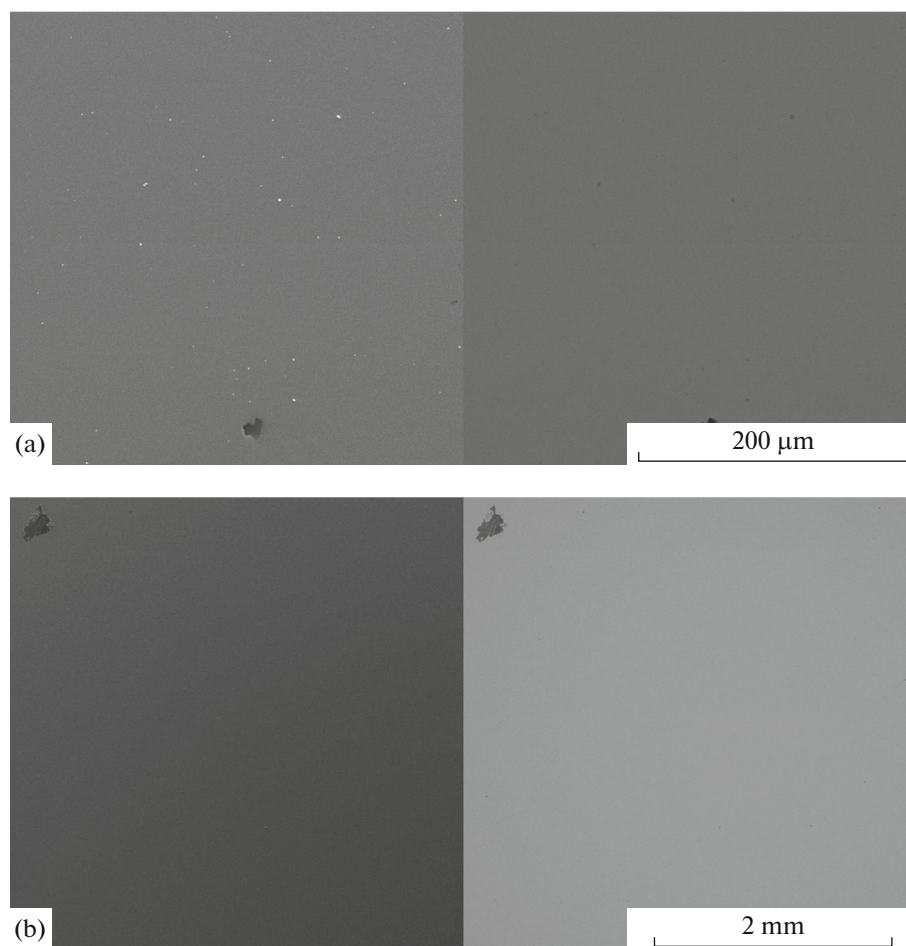


**Fig. 1.** SEM micrographs of films of metals deposited on the surfaces of silicon substrates: (a) cerium (chromium protective layer); (b) cerium (nickel protective layer). Images are presented in the mode of secondary electrons and backscattered electrons.

## TECHNIQUES OF STUDYING THE FILMS

### *X-ray Diffraction (XRD)*

The X-ray diffraction of the samples of the obtained films was performed with a Rigaku SmartLab X-ray diffractometer (Rigaku Corporation, Japan) with  $\text{CuK}\alpha$  ( $\lambda = 1.5406 \text{ \AA}$ ) anode emission within the range of angles  $2\theta = 5^\circ\text{--}60^\circ$ . The data were refined by the Rietveld method.

### *Electron Microprobe Analysis (EMPA)*

The elemental microanalysis of the surfaces of the obtained films was carried out using a SEM LEO EVO

50 XPV microscope (Carl Zeiss, accelerating voltage of 20 kV, resolution to 2 nm). Images of the regions subjected to elemental analysis were made in the mode of backscattered electrons (BSE) and secondary electrons (SE).

### *Scanning Electron Microscopy (SEM)*

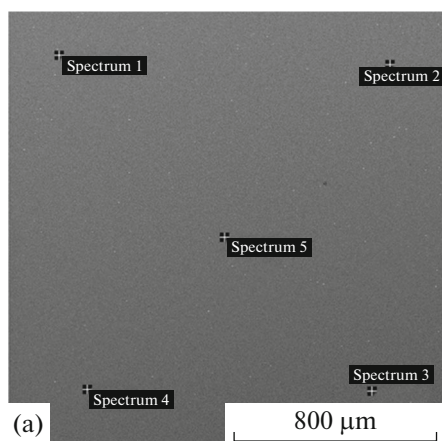
To obtain photomicrographs of the samples of the obtained films, a TESCAN VEGA scanning electron microscope with  $\text{LaB}_6$  cathode (working accelerating voltage of 30 kV, resolution to 2 nm) was used. The morphology of the samples was determined in the

**Table 1.** Cell parameters of the phases present in the composition of the cerium film (nickel protective layer) deposited on the silicon substrate after its hydrogen charging (according to the data from XRD)

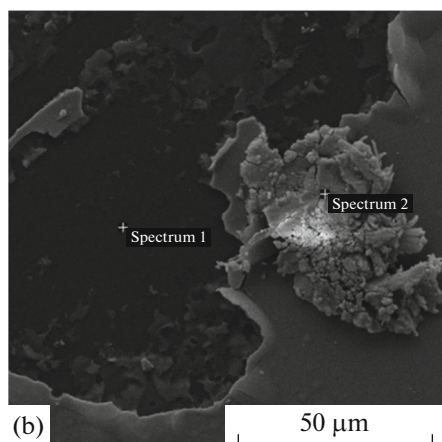
Composition	Structure	Unit cell parameter $a$ , $\text{\AA}$
$\text{CeH}_{2.51}$	FCC	$5.41 \pm 0.001$
Ni	FCC	$3.49 \pm 0.01$
Si	FCC	5.43

**Table 2.** Cell parameters of the phases present in the composition of the cerium film (chromium protective layer) deposited on the silicon substrate after its hydrogen charging (according to the data from XRD)

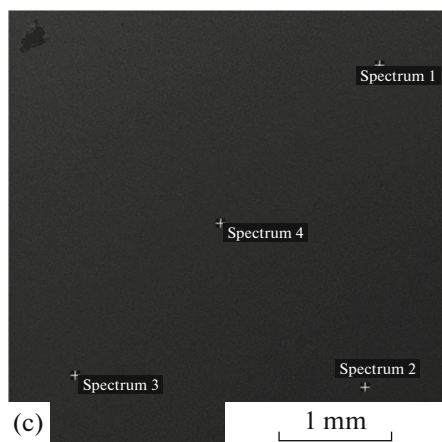
Composition	Structure	Unit cell parameter $a$ , $\text{\AA}$
$\text{CeH}_{2.51}$	FCC	$5.42 \pm 0.001$
Cr	FCC	$2.90 \pm 0.005$
Si	FCC	5.43



Spectrum	O	Si	Ce	Cr
Spectrum 1	28.22	3.68	62.72	5.38
Spectrum 2	27.58	3.64	63.22	5.56
Spectrum 3	27.31	3.71	63.35	5.63
Spectrum 4	27.64	3.84	62.89	5.64
Spectrum 5	27.75	3.74	63.13	5.38



Spectrum	Si	Cl	K	Ni	Ce
Spectrum 1	100				
Spectrum 2	4.98	1.06	0.54	9.41	84.01



Spectrum	O	Si	Ni	Ce
Spectrum 1	21.73	2.76	7.49	68.02
Spectrum 2	21.94	2.64	7.14	68.28
Spectrum 3	22.25	2.56	6.86	68.34
Spectrum 4	22.75	2.51	7.04	67.69

**Fig. 2.** Data of electron microprobe analysis of films of metals deposited on the surfaces of silicon substrates: (a) cerium (chromium protective layer); (b) cerium (nickel protective layer).

mode of secondary electrons and backscattered electrons.

### RESULTS AND DISCUSSION

Cerium is subjected to rapid oxidation under storage in air; for this reason, the films of this metal should be protected by a layer of another metal. The surfaces

of the cerium films were coated with chromium and nickel. The thicknesses of the protecting layers were 70 and 20 nm for chromium and nickel, respectively.

The SEM micrographs of the obtained films are shown in Fig. 1. In all cases, regardless of the nature of the protective metal, these films constitute a layer homogeneous over its thickness, evenly covering the whole surface of the substrate. There are only a small

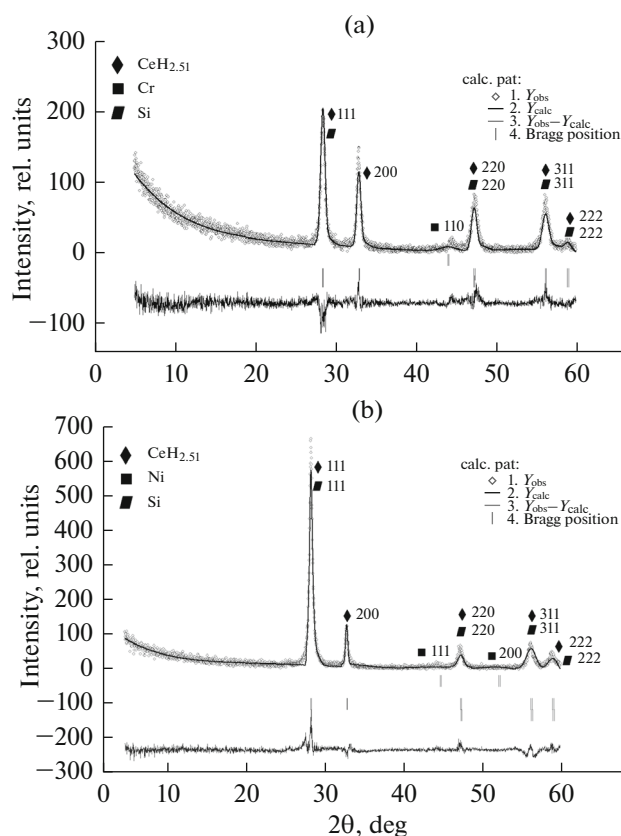


**Fig. 3.** Typical X-ray diffraction pattern of cerium films deposited on silicon substrate after hydrogen charging: (a) with chromium protective layer; (b) with nickel protective layer.

number of defects, and most of them pertain to edge defects. It can be inferred that the magnetron sputter deposition is a good method for deposition of such layers.

Composition of the deposited films was also verified by the electron microprobe analysis (Fig. 2) of several sites of the surface of each sample and by X-ray diffraction. In particular, the elemental analysis reveals that, within the area of a defect of the film (see Fig. 2b), only silicon exists, though beyond its limits the surface is represented by cerium and nickel. This supports the conclusions of uniformity of deposition of the metal at sputtering. Since the protective film of nickel and chromium has a much smaller thickness in comparison with the target metal, the material of the protective coating is not always determined in the elemental analysis. In this case, we form an opinion about the uniformity of its deposition indirectly by the contrast ratio by comparison with those analyzed sites of the surface where the metal of the protective layer is found. The composition of the deposited layers is confirmed also by the data of X-ray diffraction.

The X-ray diffraction patterns of the samples of the cerium films with the protective layer deposited on the silicon wafers and subjected to hydrogen charging are given in Fig. 3. Analysis of the diffraction pattern

demonstrates that hydrogen charging in both cases results in formation of hydride of  $CeH_{2.51}$  composition, which crystallizes in the FCC phase with the parameter  $a \approx 5.42 \text{ \AA}$  (Tables 1, 2). Also, the lines corresponding to the phase of silicon, which is the material of the substrate, are in evidence on the X-ray diffraction patterns. At the same time, reflections of phases of the metals—materials of protective coatings—are barely distinguishable from the background, which is due to their small thickness. The results of the quantitative X-ray diffraction analysis are presented in Tables 1 and 2. Note that, because of small thickness of the deposited layers, the values of lattice periods of the detected phases calculated with using the Rietveld method have a large error.

## CONCLUSIONS

Synthesis of cerium hydride films deposited on silicon was accomplished. For this purpose, first, the silicon wafers were coated with a cerium layer 300 nm thick by magnetron sputtering and then with a protective film of nickel or chromium 20 nm and 70 nm thick, respectively. Through the use of the treatment with atomic hydrogen obtained by dissociation on tungsten wire, obtaining the hydride of  $CeH_{2.51}$  com-

position under the mild conditions was a success. The utilized method of hydrogen charging of films can be used for introduction of hydrogen also into other hydride-forming metals and alloys.

#### FUNDING

This work was supported by the Russian Foundation for Basic Research, project no. 19-08-00452/19 of January 9, 2019.

#### REFERENCES

1. Notten, P., Electrochromic metal hydrides, *Curr. Opin. Solid State Mater. Sci.*, 1999, vol. 4, no. 1, pp. 5–10.
2. Khazaeli, A., Falahati, H., and Barz, D.P.J., Electrochemical investigation and modeling of  $\text{LaNi}_{4.77}\text{Al}_{0.3}$  thin-films sputtered on glass wafers, *J. Alloys Compd.*, 2019, vol. 772, pp. 199–208.
3. Guglya, A. and Lyubchenko, E., Thin film hydrogen storages, in *Handbook of Ecomaterials*, New York: Springer-Verlag, 2019, pp. 913–939.
4. Badun, G.A., Chernysheva, M.G., and Ksenofontov, A.L., Increase in the specific radioactivity of tritium-labeled compounds obtained by tritium thermal activation method, *Radiochim. Acta*, 2012, vol. 100, pp. 401–408. <https://doi.org/10.1524/ract.2012.1926>
5. Badun, G.A., Chernysheva, M.G., Yakovlev, R.Yu., Leonidov, N.B., Semenenko, M.N., and Lisichkin, G.V., A novel approach radiolabeling detonation nanodiamonds through the tritium thermal activation method, *Radiochim. Acta*, 2014, vol. 102, no. 10, pp. 941–946. <https://doi.org/10.1515/ract-2013-2155>
6. Badun, G.A., Chernysheva, M.G., Grigorieva, A.V., Eremina, E.A., and Egorov, A.V., Langmuir hydrogen dissociation approach in radiolabeling carbon nanotubes and graphene oxide, *Radiochim. Acta*, 2016, vol. 104, no. 8, pp. 593–599. <https://doi.org/10.1515/ract-2015-2516>
7. Khmel'nitsky, R.A., Evlashin, S.A., Martovitsky, V.P., Pastchenko, P.V., Dagesian, S.A., Alekseev, A.A., Suetin, N.V., and Gippius, A.A., Heteroepitaxy of Ni-based alloys on diamond, *Cryst. Growth Des.*, 2016, vol. 16, no. 3, pp. 1420–1427.

*Translated by G. Levina*